TraR directly regulates transcription initiation by mimicking the combined effects of the global regulators DksA and ppGpp

Saumya Gopalkrishnan[a], Wilma Ross[a], Albert Y. Chen[a], and Richard L. Gourse[a,1]

[a]Department of Bacteriology, University of Wisconsin–Madison, Madison, WI 53706

Edited by Jeffrey W. Roberts, Cornell University, Ithaca, NY, and approved June 6, 2017 (received for review March 11, 2017)

The *Escherichia coli* F element-encoded protein TraR is a distant homolog of the chromosome-encoded transcription factor DksA. Here we address the mechanism by which TraR acts as a global regulator, inhibiting some promoters and activating others. We show that TraR regulates transcription directly in vitro by binding to the secondary channel of RNA polymerase (RNAP) using interactions similar, but not identical, to those of DksA. Even though it binds to RNAP with only slightly higher affinity than DksA and is only half the size of DksA, TraR by itself inhibits transcription as strongly as DksA and ppGpp combined and much more than DksA alone. Furthermore, unlike DksA, TraR activates transcription even in the absence of ppGpp. TraR lacks the residues that interact with ppGpp in DksA, and TraR binding to RNAP uses the residues in the β′ rim helices that contribute to the ppGpp binding site in the DksA–ppGpp–RNAP complex. Thus, unlike DksA, TraR does not bind ppGpp. We propose a model in which TraR mimics the effects of DksA and ppGpp together by binding directly to the region of the RNAP secondary channel that otherwise binds ppGpp, and its N-terminal region, like the coiled-coil tip of DksA, engages the active-site region of the enzyme and affects transcription allosterically. These data provide insights into the function not only of TraR but also of an evolutionarily widespread and diverse family of TraR-like proteins encoded by bacteria, as well as bacteriophages and other extrachromosomal elements.

TraR | bacterial transcription initiation | RNA polymerase | ppGpp/DksA | F element

It is becoming increasingly clear that small proteins can play important regulatory roles in bacteriophage and bacterial biology (1, 2). A case in point is TraR, a 73-amino acid protein encoded in the transfer region operon (*tra*) of the *Escherichia coli* conjugative F plasmid (3). TraR shares 29% sequence identity with the C-terminal half of DksA (4), a 151-residue protein that binds to and regulates transcription initiation by *E. coli* RNA polymerase (RNAP) at specific promoters (5–7). TraR also shares homology with predicted proteins of similar length elsewhere in the bacterial sequence database that are encoded by conjugative plasmids and bacteriophages (e.g., phages 186, P2, and lambda) (8, 9).

TraR is expressed from the Py promoter as part of the major *tra* operon transcript (10). However, insertion mutations in *traR* did not alter the efficiency of F element DNA transfer, making its role in conjugation unclear (3). Herman and colleagues showed that TraR complements a Δ*dksA* mutant strain when expressed from its natural *tra* operon promoter on a conjugative plasmid or ectopically from a *trp-lac* promoter on a standard expression plasmid (4), and it activates transcription by RNAP containing the alternative σ factor, σ^E (11). Because $E\sigma^E$ activity is up-regulated by perturbations of the outer membrane and transcribes genes whose products (chaperones and proteases) alleviate membrane stress, it was suggested that TraR helps mediate a response to disruptions of the cell membrane caused by assembly of the conjugation pilus and DNA transfer apparatus (11).

TraR also affects transcription initiation by the primary holoenzyme, $E\sigma^{70}$. Like the transcription factor DksA, TraR inhibits transcription from the rRNA promoter *rrnB* P1 in vivo and in vitro, and it activates transcription from the $E\sigma^{70}$-dependent amino acid biosynthesis promoter p*livJ* in vivo (4). However, it was unclear whether activation of transcription by TraR was direct or indirect.

DksA directly inhibits transcription in the absence of the "second messenger" ppGpp in vitro, but it functions synergistically with ppGpp to inhibit transcription to a much greater extent (5). The effects of ppGpp on transcription inhibition are mediated by two binding sites ∼60 Å apart on RNAP, one at the interface of the β′ and ω subunits (site 1) (12, 13), and one at the interface of β′ and DksA in the RNAP secondary channel (site 2) (14). Only site 2 plays a role in activation of transcription, explaining why both DksA and ppGpp are required for positive control (7, 14). Because ppGpp concentrations change dramatically in response to a variety of nutritional stresses, DksA and ppGpp together coordinate transcription with the translational status of the cell, even though DksA concentrations remain relatively constant with the growth phase (15).

In this study, we provide information about the mechanism of TraR function. We show that TraR is much more active in modulating transcription than DksA alone, even though it binds to the RNAP secondary channel with only slightly higher affinity. We also show that TraR inhibits or activates a number of $E\sigma^{70}$-dependent promoters in vitro, its activity is not affected by ppGpp binding at site 1, and unlike DksA, it does not create a binding site for ppGpp analogous to site 2. We describe a model for TraR action in which TraR mimics the combined effects of ppGpp and DksA by using the residues in RNAP that help form ppGpp site 2. TraR adds to the growing repertoire of known factors—including DksA, GreA, GreB, and Rnk (15–20)—that target the β′ rim helices of RNAP to modulate transcriptional output. Members of the TraR class of

Significance

TraR is a 73-amino acid protein encoded in the transfer region operon (*tra*) of the *Escherichia coli* conjugative F plasmid. Here we describe evidence for a model in which TraR mimics the combined regulatory activities of the transcription factor DksA and the second messenger ppGpp. By interacting with the residues in RNA polymerase that form a ppGpp binding pocket, we suggest that TraR provides a means for regulating transcription initiation by targeting the secondary channel even under conditions that do not result in induction of ppGpp. TraR-like proteins appear to be ubiquitous in bacteria even in phyla distant from the proteobacteriaceae, in support of the accumulating evidence that very small proteins can have a large impact on bacterial biology.

Author contributions: S.G., W.R., and R.L.G. designed research; S.G., W.R., and A.Y.C. performed research; S.G., W.R., and A.Y.C. contributed new reagents/analytic tools; S.G., W.R., A.Y.C., and R.L.G. analyzed data; and S.G., W.R., and R.L.G. wrote the paper.

The authors declare no conflict of interest.

This article is a PNAS Direct Submission.

[1]To whom correspondence should be addressed. Email: rgourse@bact.wisc.edu.

This article contains supporting information online at www.pnas.org/lookup/suppl/doi:10.1073/pnas.1704105114/-/DCSupplemental.

regulators are present in diverse bacterial species and are encoded by a large family of phages and extrachromosomal elements.

Results

TraR Is More Active than DksA in Direct Inhibition of Transcription in Vitro, but It Has a Similar Affinity for RNAP. TraR inhibits transcription from *rrnB* P1 (Fig. 1*A*). The IC_{50} for inhibition by purified TraR in vitro was ∼50 nM, compared with ∼1.3 μM for inhibition by DksA alone, a difference of 26-fold (Fig. 1*B*). TraR was also more active than DksA for inhibition of the *rpsT* P2 promoter (for ribosomal protein S20), another promoter previously shown to be inhibited by DksA (21) (Fig. S1 *A* and *B*). The effect of TraR was promoter-specific; TraR did not inhibit transcription from the plasmid-encoded *RNA-I* promoter or the *lacUV5* promoter (Fig. 1 *A* and *B* and Fig. S2*A*).

To determine whether TraR binds to the secondary channel of RNAP, like DksA, we used a cross-linking approach. TraR-^{32}P-HMK or ^{32}P-HMK-DksA were incubated with RNAPs containing the cross-linkable amino acid Bpa substituted for β′ trigger loop residues Q929 or R933, or for β′ R1148, a position outside of the secondary channel, as a control. Previously, we found that β′ R933-Bpa cross-linked to DksA (16). β′ R933-Bpa cross-linked to both DksA and TraR, but Fig. 1*C* shows that β′ Q929-Bpa cross-linked more efficiently to DksA than to TraR.

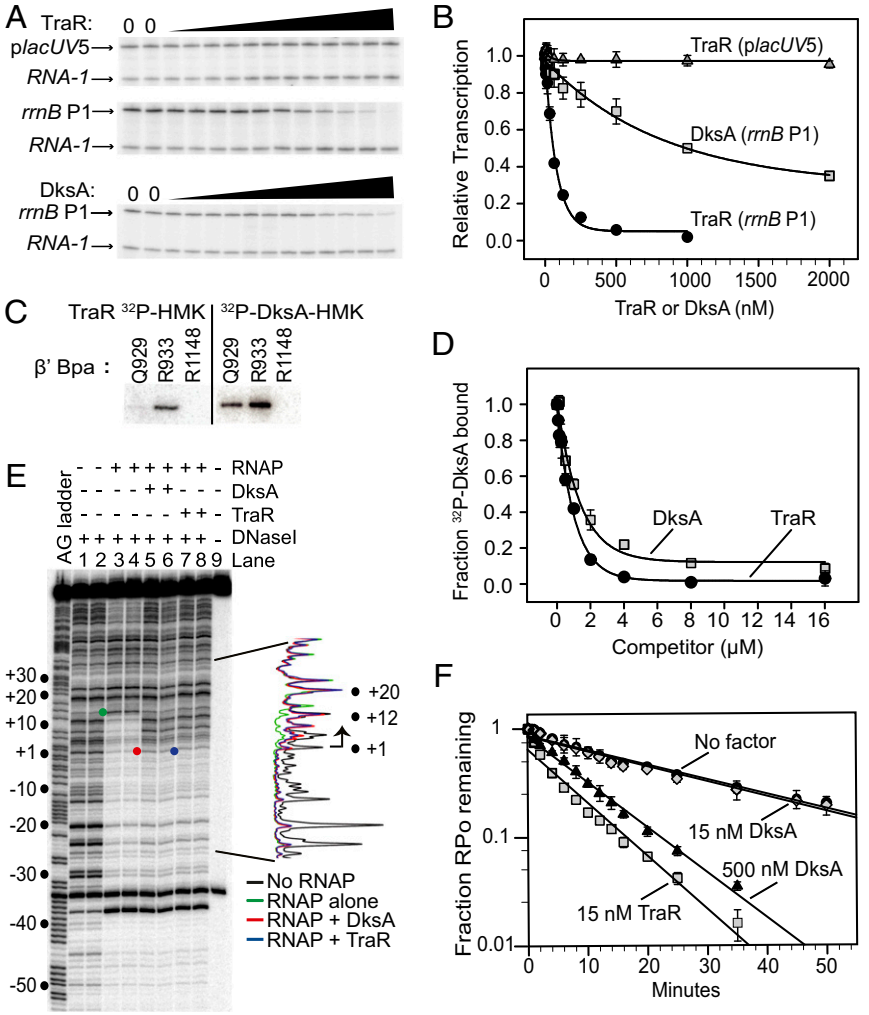

Fig. 1. TraR is more active than DksA for inhibition of transcription but has a similar affinity for RNAP. (*A*) Multiround in vitro transcription of *rrnB* P1 or *lacUV5* at a range of concentrations of TraR (wedge indicates 1 nM to 1 μM for *rrnB* P1 or 1 nM to 2 μM for *lacUV5*) or of DksA (wedge indicates 4 nM to 8 μM). Plasmid templates also contained the *RNA-1* promoter. (*B*) Quantification of transcripts from experiments like those in *A* plotted relative to values in the absence of TraR or DksA. The IC_{50} for inhibition by TraR was ∼50 nM and for DksA ∼1.3 μM [averages with SDs from at least three independent experiments (n = 3)]. (*C*) Cross-linking with β′ R933-Bpa RNAP, β′ Q929-Bpa RNAP, or β′ R1148-Bpa RNAP with ^{32}P-TraR or ^{32}P-DksA. The portion of a representative 4–12% SDS gel containing the cross-linked β′-DksA or β′-TraR products is shown. (*D*) Unlabeled DksA or TraR competes similarly for binding of ^{32}P-labeled HMK-DksA to RNAP. Unlabeled DksA or TraR (0–16 μM) was added to 1 μM ^{32}P-DksA and 0.1 μM core RNAP before Fe^{2+}-mediated cleavage of DksA. Fraction of ^{32}P-DksA cleaved was normalized to that in the absence of competitor. Next, 1 μM unlabeled DksA or 0.6 μM unlabeled TraR reduced cleavage of 1 μM ^{32}P-DksA by ∼50% (n = 3). (*E*) Representative gel showing DNase I footprints of RNAP bound to the *rrnB* P1 promoter, 3′ end-labeled on the template strand, with or without TraR or DksA. DNase I digested fragment without RNAP or added factors (lanes 1 and 2), with RNAP alone (lanes 3 and 4), with RNAP + 5 μM DksA (lanes 5 and 6), or with RNAP and 5 μM TraR (lanes 7 and 8). Undigested fragment (lane 9). A+G sequence ladder is on the *Left*. Traces of gel lanes showing extent of protection are on the *Right*. Colored dots indicate the downstream boundary of DNase I protection without (green dot; ∼+12), or with (red or blue dots; ∼+1) DksA or TraR. The upstream boundary of protection in lanes 3–8 is ∼−59 (n = 3). (*F*) TraR and DksA alter the lifetime of *rrnB* P1(dis) promoter complexes in vitro. RNAP–promoter complexes were preformed with TraR (15 nM) or DksA (15 nM or 500 nM), or without factors, and the fraction remaining at the indicated times after heparin addition was determined by transcription. Half-lives of *rrnB* P1(dis) complexes: no added factor, 18 min; 15 nM TraR, 3 min; 15 nM DksA, 18 min; 500 nM DksA, 6 min. Error bars indicate the range from two independent experiments (n = 2).

β′ R1148-Bpa did not cross-link to either DksA or TraR. These results suggest that TraR binds in close proximity to the trigger loop of RNAP but its precise position in the channel may be slightly different from DksA.

We next used a competition assay to determine whether TraR's greater effect on transcription inhibition compared with DksA resulted from a higher affinity for RNAP. Binding of ^{32}P-labeled DksA to RNAP was assessed in the presence or absence of competing unlabeled DksA or TraR using an Fe^{2+} cleavage assay in which ferrous iron was substituted for the active site Mg^{2+} in RNAP to generate hydroxyl radicals upon addition of DTT. The hydroxyl radicals cleave bound full-length ^{32}P-labeled DksA (151 residues) in the tip region, producing an N-terminal product of ∼73 residues. The 1 μM unlabeled DksA inhibited cleavage of 1 μM ^{32}P-DksA by 50%, as expected (22), whereas 0.6 μM TraR was sufficient to inhibit cleavage of ^{32}P-DksA by 50% (Fig. 1*D*). These data suggest that the apparent affinity of TraR for RNAP is only slightly greater than that of DksA, insufficient to account for the ∼26-fold lower IC_{50} for transcription inhibition of *rrnB* P1 by TraR (Fig. 1*B*).

TraR Shifts Occupancy of the RNAP–Promoter Complex to an Earlier Kinetic Intermediate and Decreases Complex Lifetime. To determine whether TraR, like DksA, inhibits transcription by reducing open complex occupancy, we compared the effects of TraR and DksA on DNase I footprints of RNAP on *rrnB* P1 (Fig. 1*E*). RNAP protected promoter DNA to ∼+12 with respect to the transcription start site (+1). Addition of DksA shifted the downstream boundary of protection back to ∼+1, consistent with our previous observations (23). TraR also shifted the downstream boundary of the complex from ∼+12 to ∼+1. At the ribosomal protein promoter, *rpsT* P2, DksA and TraR each shifted the downstream boundary of the complex from ∼+20 to ∼+5 (Fig. S1*C*). We infer that TraR and DksA have similar effects on promoter complex formation, shifting occupancy from a kinetic intermediate in which there is protection well downstream of the transcription start site to an earlier intermediate with a boundary of protection much closer to the transcription start site.

DksA reduces the half-lives of open complexes formed by all promoters, and it inhibits transcription from those promoters that make intrinsically short-lived complexes (5, 23). To facilitate comparing rate measurements of complexes with DksA vs. TraR, we used the *rrnB* P1(dis) promoter, a variant that forms more stable complexes than *rrnB* P1. At a concentration of 15 nM of each protein, the effect of TraR on promoter complex lifetime was much greater than for DksA (Fig. 1*F*). Over 30-fold more DksA (500 nM) than TraR (15 nM) was required to reduce promoter complex half-life to the same extent (Fig. 1*F*). These results are consistent with the much greater effects of TraR than DksA on transcription inhibition (Fig. 1 *A* and *B*).

TraR Directly Activates Transcription by $E\sigma^{70}$ in Vitro. Although it was shown previously that TraR stimulates transcription from a positively regulated promoter in vivo, even in a strain lacking ppGpp (4), this activation could have been indirect, resulting from direct inhibition of rRNA transcription by TraR, leading to a subsequent increase in the availability of RNAP and thus increased occupancy of promoters subsaturated for RNAP (24). To address whether the effect of TraR was direct, we measured whether it increased the activities of several amino acid biosynthesis or transport promoters in vitro that were shown previously to be activated by DksA and ppGpp together (7). TraR increased transcription from the *argI*, *thrABC*, *hisG*, and *livJ* promoters three- to fourfold; half-maximal activation was achieved at ∼50 nM TraR (Fig. 2 *A* and *B* and Fig. S2*A*), similar to the concentration required for inhibition of *rrnB* P1 (Fig. 1 *A* and *B*). Activation by TraR was promoter-specific: Under the same conditions, TraR had no effect on the *lacUV5* promoter (Figs. 1 *A* and *B* and 2*B*) and only a small (∼twofold) effect on the *RNA-1* promoter (Fig. S2*A*). In contrast to its requirement for activation by DksA, ppGpp was not required for activation by TraR (Fig. 2 *C* and *D*). TraR also activates the σ^E-dependent *rpoH* P3 promoter without ppGpp (11).

The degree of activation by TraR and DksA/ppGpp was not always the same. On the promoter for the small RNA, DsrA (25), and on the promoter for the antiadapter protein, IraP (26), TraR had a smaller effect than ppGpp/DksA (Fig. 2*E* and Fig. S2*B*).

TraR Functions Independently of ppGpp. ppGpp binds to two sites on RNAP, one at the interface of the β′ and ω subunits (site 1) and one at the interface of DksA and the rim helices of β′ (site 2) (14). We used a DRaCALA (differential radial capillary action of ligand) assay (27), which measures binding of ^{32}P-ppGpp directly (*Materials and Methods*), to ask whether TraR creates a ppGpp binding site analogous to site 2, the site created by DksA (Fig. 3 *A* and *B*). In the absence of DksA, ppGpp bound to WT RNAP (Fig. 3 *A*, *i*), and it did not bind to RNAP lacking the ω subunit (Δω RNAP; i.e., lacking site 1) (Fig. 3 *A*, *ii*). However, ppGpp bound to Δω RNAP when DksA was included, creating site 2 (Fig. 3 *A*, *iii*). As expected, addition of 1 mM nonradioactive ppGpp competed with binding of the radio-labeled ppGpp (Fig. 3 *A*, *iv*). ^{32}P-ppGpp did not bind to Δω RNAP when as much as 10 μM TraR was included (Fig. 3 *A*, *v*–*vii*), nor did ^{32}P-ppGpp bind to purified TraR without RNAP (Fig. 3 *A*, *ix*). We conclude that TraR does not create a ppGpp binding site on RNAP analogous to site 2, and it does not bind ppGpp by itself.

Consistent with the lack of a TraR-dependent ppGpp binding site (Fig. 3 *A* and *B*), inhibition of transcription by TraR did not require ppGpp and was only slightly stronger in the presence of ppGpp. With WT RNAP, TraR (60 nM) inhibited *rrnB* P1 ∼threefold in the absence of ppGpp, and ppGpp by itself inhibited *rrnB* P1 ∼two- to threefold (Fig. 3*C*), consistent with our previous results (12). When both TraR and ppGpp were added to WT RNAP together, *rrnB* P1 was inhibited ∼fivefold, reflecting an additive effect of the two factors. The additional effect from ppGpp was not observed with Δω RNAP, indicating that it derived from ppGpp binding to site 1.

The extent of inhibition of *rrnB* P1 transcription varied with TraR concentration (Figs. 1*B* and 3*D*), and was the same, relative to reactions without TraR, in either the presence or the absence of ppGpp (Fig. 3*D*) (IC_{50} ∼50–55 nM). In contrast, the extent of inhibition by DksA was greatly amplified by ppGpp, consistent with our previous results (5, 14) (Fig. 3*D*). TraR inhibited *rrnB* P1 much more than DksA alone, and at least as much as DksA and ppGpp together. Thus, TraR is insensitive to the presence of ppGpp and functionally mimics the effects of DksA and ppGpp together.

Strains lacking either ppGpp or DksA or both are unable to grow on medium lacking amino acids (4, 5). Uninduced levels of TraR expressed from pTrc99a were sufficient to complement strains lacking DksA or both DksA and ppGpp (Fig. 3*E*, sectors 1 and 3), but longer incubation times (Fig. 3*F*, sector 2) or induced (higher) levels of TraR (Fig. 3*G*, sector 2) were required to complement the strain lacking only ppGpp. It is possible that DksA competes with TraR for the secondary channel in the Δ*relA*Δ*spoT* strain, resulting in a requirement for higher TraR levels to complement the ppGpp defect. Taken together, our data suggest that TraR mimics the effect of ppGpp and DksA together in vitro and when supplied ectopically in vivo, and that ppGpp does not affect TraR function (Figs. 2 *C* and *D* and 3 *D*–G).

TraR and DksA Interact Differently with the Same Part of RNAP. TraR's higher activity than DksA and its ppGpp-independence (Figs. 1–3) and the observation that β′ Q929-Bpa cross-linked much more efficiently to DksA than to TraR (Fig. 1*C*) suggest that there are differences in the way TraR and DksA interact with RNAP. No high-resolution structural information is available for DksA bound

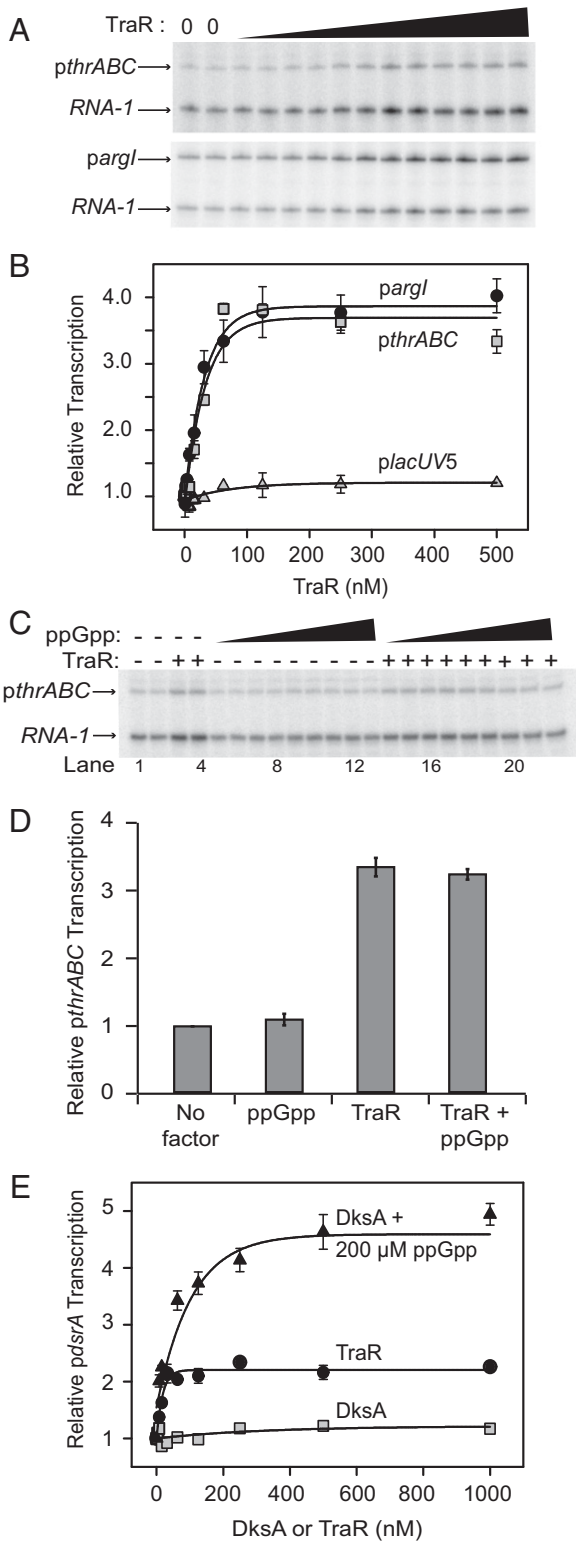

Fig. 2. TraR activates transcription by $E\sigma^{70}$ at DksA/ppGpp-regulated promoters. (*A*) Representative gel images showing multiple round transcription from the *thrABC* or *argI* promoters in the presence of increasing concentrations of TraR (0–2 μM) indicated by a wedge. (*B*) Quantification of data as in *A* (n = 3). Transcription was normalized to that in the absence of TraR. *lacUV5* promoter is shown for comparison (gel image is in Fig. 1*A*). (*C*) Representative gel image showing transcription from p*thrABC* with TraR (500 nM), ppGpp (1.5–400 μM), or TraR (500 nM) and ppGpp (1.5–400 μM). (*D*) Quantification of data for ppGpp alone (200 μM), TraR alone (500 nM), or TraR (500 nM) + ppGpp (200 μM) expressed relative to values in the absence of factors (n = 3). Error bars indicate SD. (*E*) Transcription from the *dsrA* promoter, at the indicated concentrations of DksA alone, TraR alone, or DksA + 200 μM ppGpp, relative to transcription without factor (n = 3).

to RNAP, but genetic and biochemical studies support a model in which several different parts of RNAP interact directly with DksA. These include: the β′ secondary channel rim, including residue E677, which interacts with the DksA globular domain (14, 17, 28); the RNAP active site region at the base of the secondary channel and the trigger loop, which interact with the DksA coiled-coil tip (16, 17, 29) (Fig. 1*C*); and the sequence insertion 1 (SI1) subdomain in the nearby β-subunit, which binds to the C-terminal helix of DksA (17).

When RNAP contained the β′ E677A substitution or either of two deletions in β SI1, TraR, like DksA, failed to inhibit *rrnB* P1 (Fig. 4*A*) or to activate the *thrABC* promoter (Fig. 4*B*). However, other substitutions in the rim helices (β′ N680A, K681A, or the double substitution, β′ N680A/K681A) had different effects on responses to TraR vs. DksA. The three variants were defective in responding to TraR, either for inhibition of *rrnB* P1 (Fig. 4*C*) or for activation of *thrABC* (Fig. 4*D*), whereas the same substitutions did not interfere at all with DksA function. In fact, DksA functioned slightly better with the mutant RNAPs than the WT RNAP in the absence of ppGpp. The IC_{50} ratios (mutant/WT) for inhibition of *rrnB* P1 by TraR were 4.7 for K681A RNAP, 2.4 for N680A RNAP, and 3.4 for N680A/K681A RNAP (see Fig. 4*C* legend for IC_{50} values). In contrast, the IC_{50} ratios (mutant/WT) for inhibition by DksA were 0.75 for β′ N680A, 0.83 for K681A, and 0.5 for β′ N680A/K681A RNAP (14).

Because nearly full TraR function with the β′ N680A and K681A RNAPs was observed at high TraR concentrations, it is likely that a reduction in TraR affinity was responsible for the defect in function of the rim helix variants. We suggest that DksA and TraR both bind to the rim helices, and TraR mimics the effect of DksA and ppGpp together by interacting directly with the same or nearby residues in the rim helices that help form ppGpp binding site 2.

Alignment of TraR with DksA and Analysis of Critical TraR Residues. Alignment of TraR with DksA (Fig. 5*A*) indicated some common features. First, like DksA, TraR contains two aspartates and an alanine residue near its N terminus, D3, D6, and A8, which could correspond to D71, D74, and A76, the residues near the tip of the DksA coiled-coil. Second, TraR also contains four cysteine residues, C37A, C40A, C58A, and C61A, which could correspond to the four cysteines, C114, C117, C135, and C138, that form a zinc-binding motif in the DksA globular domain (6). Consistent with this proposal, we found that zinc was present at a 1:1 molar ratio in purified WT TraR when examined by inductively coupled plasma mass spectrometry (*Materials and Methods*). Third, TraR contains an isoleucine at residue 20 (I20) that could correspond to N88 in DksA, where an N-to-I substitution strongly increased DksA binding to RNAP (30). Fourth, the C-terminal helix of DksA is critical for its interactions with RNAP, especially E143 (17). In our alignment, E66 of TraR corresponded to E143 in DksA.

To determine whether these residues in TraR were important for function, single substitutions were constructed and the variants were screened for complementation of a Δ*dksA* strain for growth on minimal medium when expressed ectopically from the pTrc99a plasmid (Table S1). We then overexpressed the variants from the T7 promoter on pET28a and purified them to analyze their RNAP binding properties and their effects on transcription in vitro (see TraR expression and purification section in *SI Materials and Methods*).

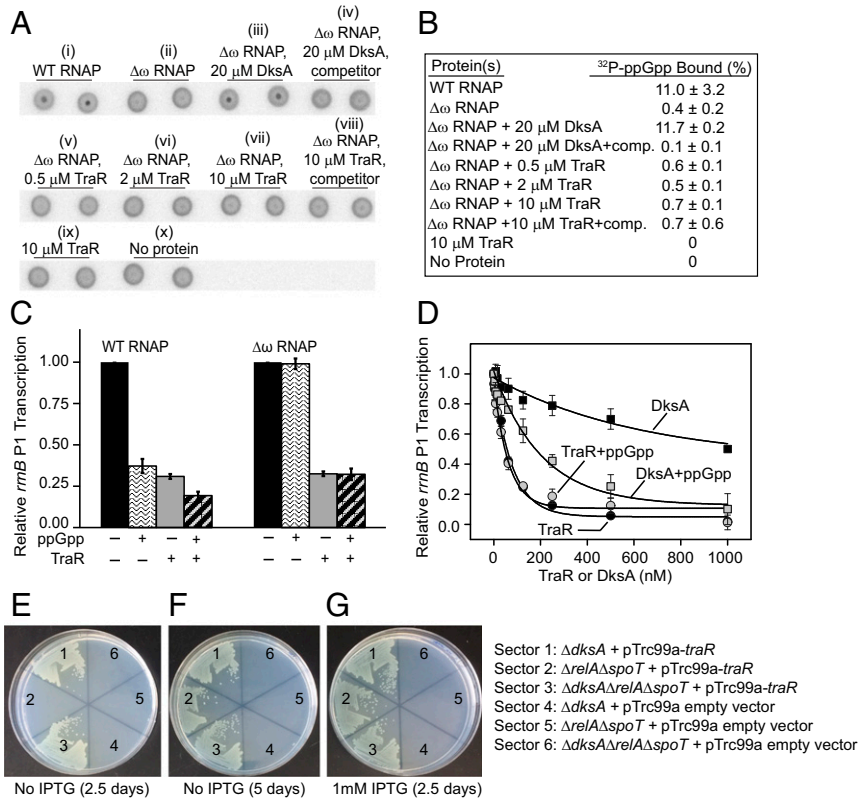

Fig. 3. TraR does not form a ppGpp binding site analogous to site 2 in the RNAP–DksA–ppGpp complex. (*A*) DRaCALA assay for ^{32}P-ppGpp binding. Duplicate filters are shown for each reaction. *Top*: (*i*) 2 μM WT RNAP (site 1); (*ii*) 2 μM Δω RNAP (lacking site 1); (*iii*) 2 μM Δω RNAP with 20 μM DksA (site 2); (*iv*) 2 μM Δω RNAP with 20 μM DksA (site 2) and 1 mM unlabeled ppGpp competitor. *Middle*: 2 μM Δω RNAP with (*v*) 0.5 μM TraR, (*vi*) 2 μM TraR, (*vii*) 10 μM TraR, or (*viii*) 10 μM TraR and unlabeled ppGpp competitor. *Bottom*: (*ix*) 10 μM TraR, no RNAP; (*x*) buffer only. (*B*) Quantification of results ($n = 2$). (*C*) Multiple round transcription of *rrnB* P1 with either WT RNAP or Δω RNAP, with 200 μM ppGpp and/or 60 nM TraR, as indicated. Quantification, expressed relative to reactions without factors ($n = 2$). (*D*) TraR mimics the effects of DksA and ppGpp together at site 2 in vivo. Transcription of *rrnB* P1 with 0–1,000 nM TraR or DksA, in reactions containing or lacking 200 μM ppGpp. Values expressed relative to no TraR or DksA added. TraR, either with or without ppGpp, inhibited transcription to the same extent as DksA + ppGpp. The IC_{50} value was ∼50–55 nM for TraR ± ppGpp, ∼1.3 μM for DksA alone, and ∼180 nM for DksA and ppGpp together. (*E–G*) Complementation of strains lacking DksA for growth on minimal medium. (*E*) No IPTG (isfopropyl-β-D-thiogalactopyranoside) (i.e., uninduced expression only), 2.5 d of incubation. (*F*) No IPTG, 5 d of incubation. (*G*) 1 mM IPTG, 2.5 d of incubation. Strains in each sector are described on the *Right*.

TraR variants with substitutions for D3, D6, or A8, the positions proposed to correspond to D71, D74, and A76 in DksA, were unable to complement a Δ*dksA* strain (Table S1). As measured by the competition assay described in Fig. 1*D*, purified D3A, D6A, and A8T TraR were only partially defective for binding to RNAP in vitro (Fig. 5*B*), yet all three variants were almost completely defective in inhibiting *rrnB* P1 and activating *thrABC*. Regulation of transcription was severely defective even at high concentrations of D3A and D6A TraR, where binding to RNAP was almost indistinguishable from WT TraR (Fig. 5 *C* and *D*; see legend for IC_{50} values). Thus, the N-terminal residues in TraR are required for function subsequent to RNAP binding. A substitution for D3 had a more severe defect in TraR function than a substitution for the analogous residue in DksA, D71 (29), indicating that TraR and DksA do not interact with RNAP identically. The defects in function of the N-terminal variants are consistent with previous reports that TraR D6N is defective for inhibition of *rrnB* P1 and *rpoH* P3-*lacZ* fusions in vivo (4, 11).

Substitutions for I20 and E66, the positions corresponding to N88 and E143 in DksA (see above), eliminated complementation of a Δ*dksA* mutant (Table S1) and were defective for inhibition and activation of transcription in vitro, even though the purified proteins retained substantial RNAP binding activity (Fig. 5). We suggest that these TraR variants bind to RNAP but they might be positioned incorrectly, accounting for the loss of function.

TraR variants with alanine substitutions at C37, C40, C58, or C61, the residues in our alignment corresponding to the Zn-binding motif in DksA (Fig. 5*A*), were unable to complement the Δ*dksA* strain for growth on minimal medium after ectopic expression from pTrc99a (Table S1). Because we were unable to purify the cysteine variants after overexpression from pET28a, we could not distinguish whether these variants had specific defects vs. defects in overall structure.

Models for TraR and the TraR–RNAP Complex. The alignment of TraR and DksA and the genetic and biochemical data on the roles of specific residues in RNAP or TraR on TraR function were used to create a model for the TraR–RNAP complex. No structural information is available for TraR, so a computational model for the structure of TraR was generated using the RaptorX web server (31) (raptorx.uchicago.edu/StructurePrediction/predict/). RaptorX chose the known structure of DksA (1TJL) (6) as a template for prediction of the TraR structure. In this model, TraR contains a long N-terminal α-helix (residues 1–29), a globular domain containing a C4-type zinc finger (residues 30–61), and a C-terminal α-helix (residues 62–73) (Fig. 6*A*). These features are similar to features in the C-terminal half of the DksA structure (Fig. 6*B*).

Our model for the TraR–RNAP complex is shown in Fig. 6*C*. The position of TraR in complex with RNAP was based on the position of DksA in our model of the DksA–RNAP complex

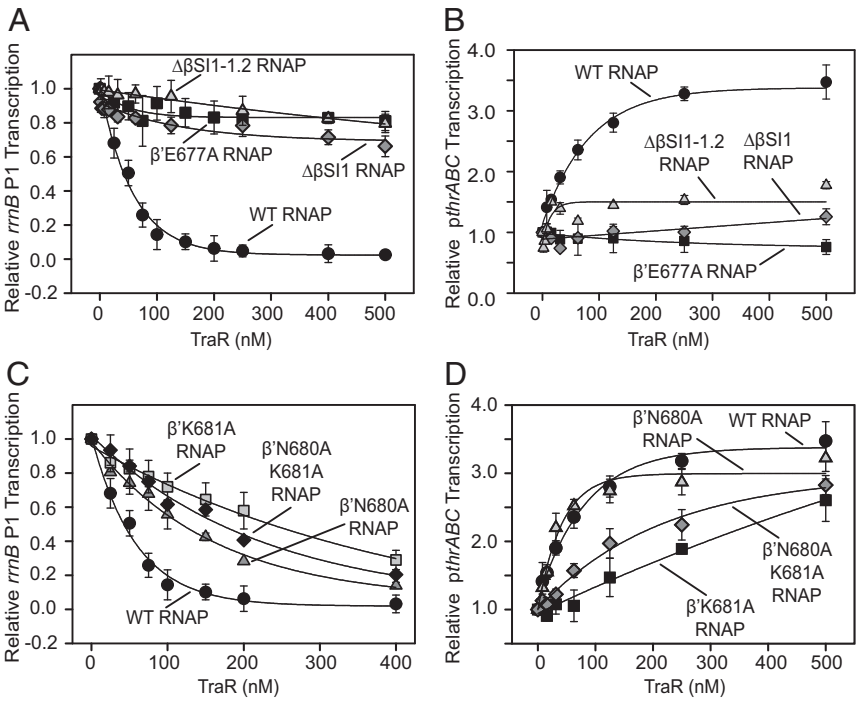

Fig. 4. RNAPs with β′ secondary channel substitutions or β SI1 deletions have defects in inhibition and activation of transcription by TraR. Each panel shows transcription relative to that without TraR. (*A*) Transcription from *rrnB* P1 by WT RNAP, β′ E677A RNAP, ΔβSI1 RNAP (*rpoB* Δ225–343), or ΔβSI1-1.2 RNAP (*rpoB* Δ240–284) with increasing concentrations of TraR (0–500 nM, $n = 3$). (*B*) Transcription from the *thrABC* promoter by WT RNAP, β′ E677A RNAP, ΔβSI1 RNAP, or ΔβSI1-1.2 RNAP with 0–500 nM TraR ($n = 3$). (*C*) Transcription from *rrnB* P1 by WT RNAP, β′ N680A RNAP, β′ K681A RNAP, or β′ N680A/K681A RNAP with 0–400 nM TraR ($n = 2$). IC_{50} for inhibition: WT RNAP, ∼50 nM; β′ N680A RNAP, ∼120 nM; β′ K681A RNAP, ∼235 nM; β′ N680A/K681A RNAP, ∼170 nM. (*D*) Transcription from the *thrABC* promoter by WT RNAP, β′ N680A RNAP, β′ K681A RNAP, or β′ N680A/K681A RNAP with 0–500 nM TraR ($n = 2$).

(14). We considered two possible alignments of TraR with DksA. In one, the globular domains and C-terminal helices of the two proteins were aligned in PyMol, but with this alignment, TraR D3, D6, and A8 and the coiled-coil tip of DksA (D71, D74, and A76) did not superimpose, because the lengths of the α-helices of TraR and DksA differed by eight to nine amino acids. In the alternative alignment, which we favor because of the importance of D3, D6, and A8 to TraR function, these N-terminal residues and the coiled-coil tip residues of DksA, as well as a portion of the adjoining α-helices, were superimposed, but the globular domains were offset because of the length difference in the α-helices (Fig. 6*B*). This alignment of TraR and DksA was used to create the model of the TraR–RNAP complex. The model of the complex is consistent with cross-linking of both DksA and TraR to Q933 in the trigger loop (16) (Fig. 1*C*) and positions the N-terminal region of TraR to make a close approach to the active site region of RNAP, like DksA (14, 16, 17).

β′ E677, N680, and K681 interact with TraR in our model of the complex, in support of the hypothesis that TraR mimics the effect of DksA and ppGpp together by interacting directly with the same β′ residues that help form ppGpp binding site 2 (Fig. 6 *D* and *E*). Consistent with the inability of ppGpp to bind to the TraR–RNAP complex (Fig. 3*A*), the N680 and K681 interaction with TraR would compete with the availability of these residues for interaction with ppGpp. Furthermore, TraR does not contain the residues corresponding to those in DksA that interact with ppGpp in site 2 (DksA L95, K98, R129, K139) (14) (Fig. 5*A*), consistent with the absence of an effect of ppGpp on TraR function.

In our model of the complex, TraR I20 is in a distorted segment of the N-terminal α-helix but it does not make direct contacts to the RNAP rim (Fig. 6 *A* and *D*). Explanations for the strong effect of the I20A variant on TraR function and for the effect of DksA N88I on binding to RNAP await further investigation. In contrast, E66 interacts directly with the rim helices (Fig. 6*A*) in the model, suggesting that effects of the E66A variant result from changes in direct contacts to RNAP.

Some parts of RNAP that likely interact with TraR are mobile, including βSI1 and the trigger loop, and thus these interactions are not illustrated. We emphasize that the lack of an experimentally determined TraR structure and the absence of some modules of RNAP with which TraR interacts makes our model of the complex speculative.

Conservation of Residues Among TraR Homologs. The degree of conservation of each TraR residue in a representative group of 100 TraR homologs was investigated using the ConSurf web server (consurf.tau.ac.il/2016/) (32). We limited analysis to ORFs of 69–75 residues (i.e., similar to the length of TraR) from a variety of bacterial, plasmid, and bacteriophage sources (Fig. 7*A* and Table S2). The five residues tested in Fig. 5 *B–D* and the four cysteines forming the putative Zn finger were among the most highly conserved residues in TraR homologs (Fig. 7*A*).

We chose eight additional residues in the globular domain of TraR for investigation in vitro based primarily on their conservation or proximity to conserved residues: P43, I44, P45, E46, A47, R48, R49, and I51 (Fig. 7 and Fig. S3). Two variants with substitutions in the putative Zn-binding domain, A47T and I51A, retained a substantial capacity to bind RNAP (Fig. 7*B*), suggesting they did not have global structural defects and yet were still functionally compromised (Fig. 7 *C* and *D*), consistent with the TraR–RNAP model (Fig. 6) in which the globular domain is proposed to interact with the β′ rim helices. Two other variants in the putative Zn-binding domain, I44A and R48A, had severe defects on RNAP binding, so without further data we cannot attribute their defects to specific rather than global effects on structure. Four other TraR globular domain variants—P43A,

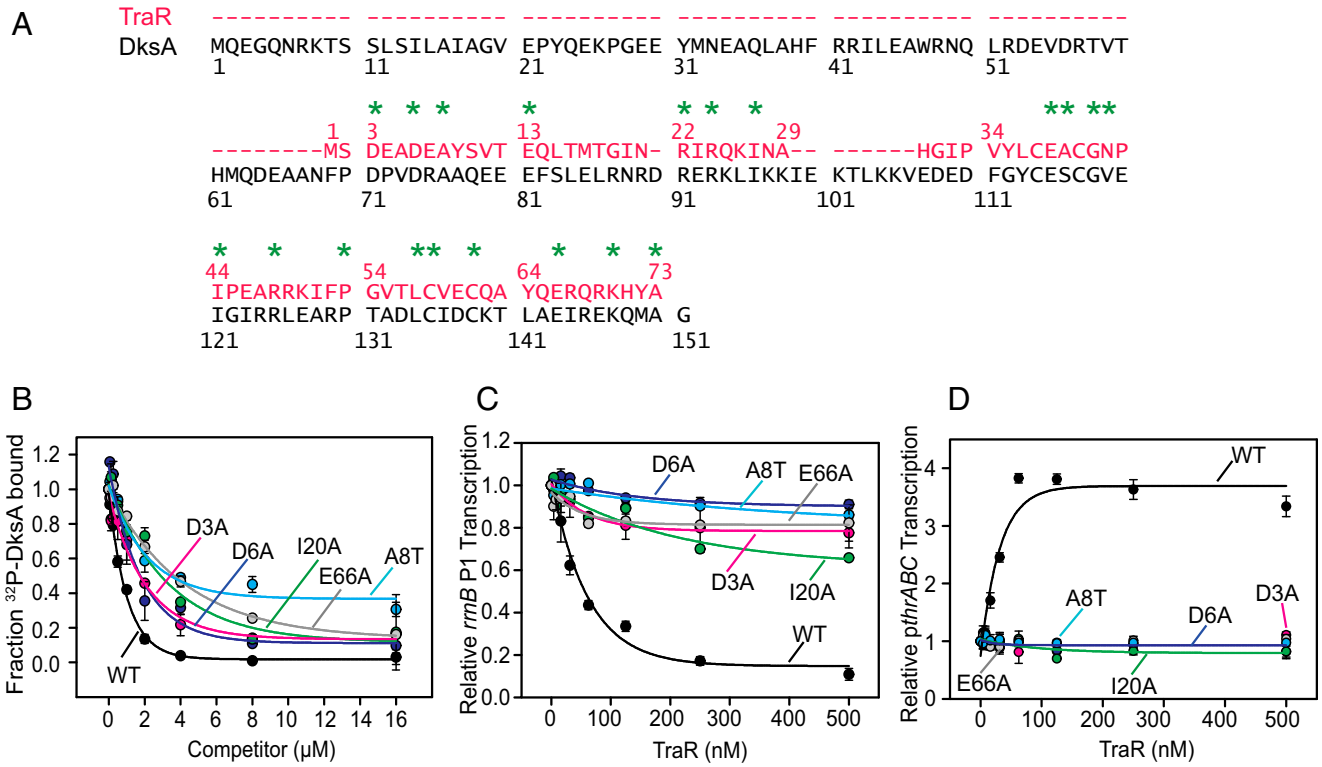

Fig. 5. Alignment of DksA and TraR and analysis of critical TraR residues. (*A*) Alignment of TraR (red) and DksA. Asterisks indicate identical residues. Dashes represent gaps. (*B*) Effects of substitutions in TraR on binding to RNAP as determined by competition with ^{32}P-DksA by Fe^{2+}-mediated cleavage ($n = 2$). 0.6 μM WT TraR, 1.75 μM D3A or D6A, 3.3 μM A8T, 2.8 μM I20A, and 3.6 μM of E66A reduced cleavage of 1.0 μM WT ^{32}P-DksA by 50%. (*C*) Inhibition of *rrnB* P1 transcription with WT RNAP as in Fig. 1, but with WT TraR and TraR variants. IC_{50} = ~55 nM for WT TraR, ~1.7 μM for D3A, ~3.3 μM for D6A, ~2.2 μM for A8T, 750 nM for I20A, ~1.8 μM for E66A ($n = 2$) (*SI Materials and Methods*). (*D*) Activation of the *thrABC* promoter as in Fig. 2 but with WT TraR and TraR variants ($n = 2$).

P45A, E46A, and R49A—functioned similarly to WT TraR both in vivo and in vitro, despite the fact that two of these residues, P45 and R49, were among the most highly conserved residues in our alignment of TraR homologs (Fig. 7*A* and Fig. S3). Twenty-five additional variants were tested by complementation analysis in vivo (Fig. S4 and Table S1). Many variants complemented, indicating that the identity of the WT residue was not essential for function.

TraR Appears to Function as a Monomer. Because TraR is only half the length of DksA, and it was reported previously that DksA variants with a shorter N-terminal tail were more active than WT DksA (33), it seemed plausible that a DksA variant consisting only of its C-terminal half (residues 69–151) (Fig. S5), the half corresponding to TraR, might be functional. When expressed from the pTrc99a vector in vivo, this "half-DksA" variant was easily detected in a Western blot (Fig. S5*A*), but it did not complement a strain lacking DksA for growth on minimal medium (Fig. S5 *B* and *C*).

Because a DksA variant consisting only of its C-terminal half was not functional, we also tested whether TraR might form a dimer, accounting for its ability to function like DksA. We measured TraR's oligomeric state directly by sedimentation equilibrium analytical ultracentrifugation (SE-AUC) and its molecular mass by electrospray ionization (ESI)-mass spectroscopy (Fig. S6*A*). In neither case was there evidence for TraR dimers. The molecular mass of purified TraR was 8,648.2 Da, consistent with a monomer lacking the N-terminal methionine and containing four extra residues (LVPR) at the C terminus remaining from the cleaved thrombin site (*Materials and Methods*).

Finally, we mixed together TraR samples with and without a His-tag. The two proteins were distinguishable by size by PAGE (Fig. S6*B*), but no untagged TraR coeluted from the nickel resin with the His-tagged protein, suggesting that TraR monomers do not associate to form dimers (Fig. S6*B*). Taken together, the SE-AUC, the ESI-mass spectrometry data, and the mixed heterodimer analysis all suggest that TraR does not form dimers in solution.

Discussion

What Accounts for the Greater Activity of TraR Relative to DksA Without ppGpp? We found that the activity of TraR was much higher than the activity of DksA in the absence of ppGpp; it inhibited transcription much more than DksA alone and it activated transcription even in the absence of ppGpp. The high activity of TraR was similar to that of DksA and ppGpp together. Because the TraR–β′ interface did not create a binding site for ppGpp analogous to the site that forms at the DksA–β′ interface, site 2, TraR was completely insensitive to ppGpp. Rather, we propose that TraR excludes binding of ppGpp to RNAP by occupying the same surface on the β′ rim helices as used by DksA to form site 2.

The extraordinary activity of TraR was not attributable to a much higher affinity for RNAP. Rather, we suggest that TraR allosterically alters the DNA binding surface in the main channel of RNAP, as proposed previously for DksA (21). For DksA, this conformational change (in the presence of ppGpp) was proposed to involve allosteric effects of an interaction of the C-terminal helix with the SI1 region the β-subunit (14). These interactions could impact interactions of the DksA coiled-coil tip aspartate residues with the trigger loop/bridge helix of RNAP, which could in turn allosterically affect promoter DNA interactions in the main channel (23, 34). Alternatively, β-subunit–SI1 interactions could affect promoter binding by altering the downstream DNA binding interface in β (34, 35). Interactions of TraR with the trigger loop/active site region and/or β SI1 would thus mimic the

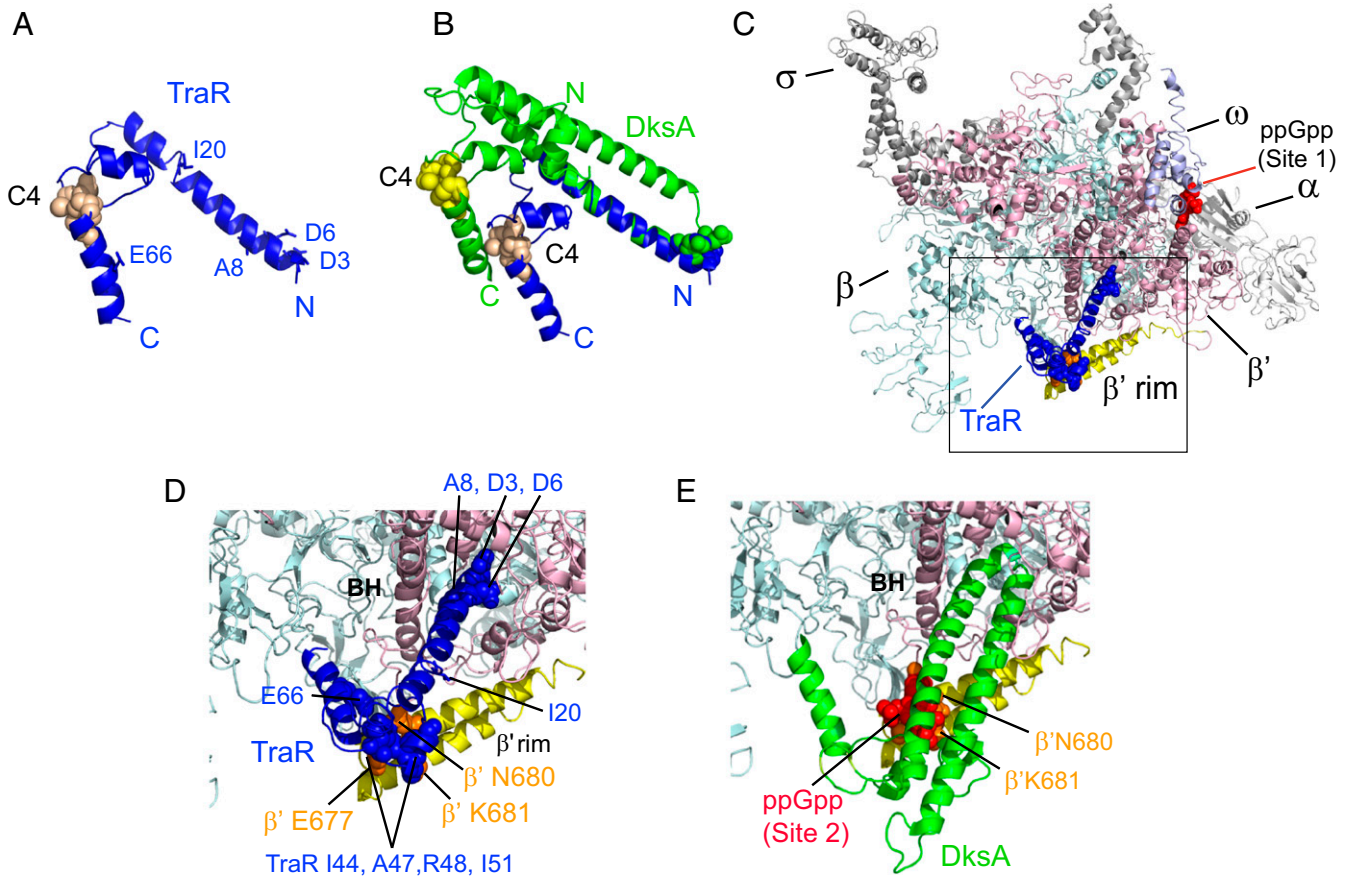

Fig. 6. Models for TraR and the TraR–RNAP complex. (*A*) RaptorX-derived model for TraR. N- and C-termini are indicated, the four cysteine residues (C4) are tan spheres, and residues D3, D6, A8, I20, and E66 are in blue stick form. (*B*) TraR (blue) and DksA (green) were positioned manually based on alignment of TraR D3, D6, and A8 with DksA D71, D74, and A76, a portion of the TraR N-terminal α-helix, and the DksA α-helix 2 in its coiled-coil. Cysteines (C4) are yellow or tan spheres. (*C*) Model for TraR binding to *E. coli* RNAP (from PDB ID code 4JKR) (14). The square corresponds to the area of the complex shown in expanded form in *D* and *E*. TraR is dark blue; the RNAP β-subunit is cyan, β′ is pink, the β′ secondary channel rim is yellow, and ω is pale blue. β′ Residues N680, K681A, and E677 are shown as orange spheres. ppGpp at site 1 is shown in red. TraR residues D3, D6, I44, A47, R48, I51, A47, and E66 are shown as blue spheres. (*D*) Enlarged view of TraR bound to RNAP secondary channel, as in *C*. I20 is in stick form. BH, bridge helix. (*E*) Complex of RNAP, DksA, and ppGpp at Site 2 (red spheres) from ref. 14.

allosteric changes caused by ppGpp binding to site 2 in the RNAP–DksA complex.

Multiple Secondary Channel Binding Proteins: Why both DksA and TraR? DksA and the Gre factors modulate *E. coli* RNAP activity by targeting the RNAP secondary channel. DksA and the Gre factors share some structural features, including a coiled-coil with conserved aspartic acid residues at the tip, but they have very little sequence similarity, very different globular domains, and perform distinct functions. GreA and GreB are transcription elongation factors that stimulate RNAP's intrinsic RNA cleavage activity to modulate escape from pauses and arrest sites during the elongation phase (18, 19). In contrast, DksA does not promote RNA cleavage (6) but rather acts to regulate transcription initiation in conjunction with ppGpp (5, 7). Although high concentrations of Gre factors can inhibit transcription initiation in vitro or when overexpressed in vivo, there is little evidence that they regulate open complex formation under physiological conditions in vivo (15). Because the Gre factors do not contain the amino acid sequences that contribute to site 2, ppGpp and the Gre factors do not synergize (15).

Unlike the functions of DksA and the Gre factors, the functions of DksA and TraR do overlap. Why then does the F element encode TraR when ppGpp/DksA already can provide the same function? Although TraR is not essential DNA transfer during conjugation (3, 10), previous studies established that it is coexpressed with other *tra* operon products from the F element Py promoter (10). Conjugation efficiency is highest in exponential growth (36), but ppGpp levels are very low during these conditions (37). We speculate that TraR's function is to regulate host promoters in the absence of ppGpp that are normally targeted by ppGpp/DksA, including rRNA promoters and amino acid biosynthesis-related promoters, but also some promoters needed for helping to mitigate membrane damage during conjugation (4, 11). Finally, because TraR and DksA/ppGpp can regulate the same promoters to different extents (Fig. 2 and Fig. S2*B*), in theory TraR could alter expression to favor conjugation, but it remains to be determined whether either ppGpp/DksA or TraR directly regulates production of specific *tra* region transcripts or whether conjugation efficiency is altered in strains lacking DksA/ppGpp.

TraR suppresses the amino acid auxotrophy of a Δ*dksA* strain when supplied from a mini-F plasmid, and we found that it regulates transcription, both negatively and positively, when expressed from the *trp-lac* promoter on pTrc99a, a standard expression plasmid, even without induction (4) (Fig. 3*E* and Table S1). Thus, a very low concentration of TraR appears to be sufficient to regulate transcription in vivo. In fact, we were unable to detect TraR in Western blots under this condition. Because 1 ng was the lowest amount of purified TraR that we could detect in Western blots, and we could not detect a comparable TraR signal even with as much as 15 μg of cell lysate loaded per lane, we estimate that there is <1 ng of TraR in 15 μg of total

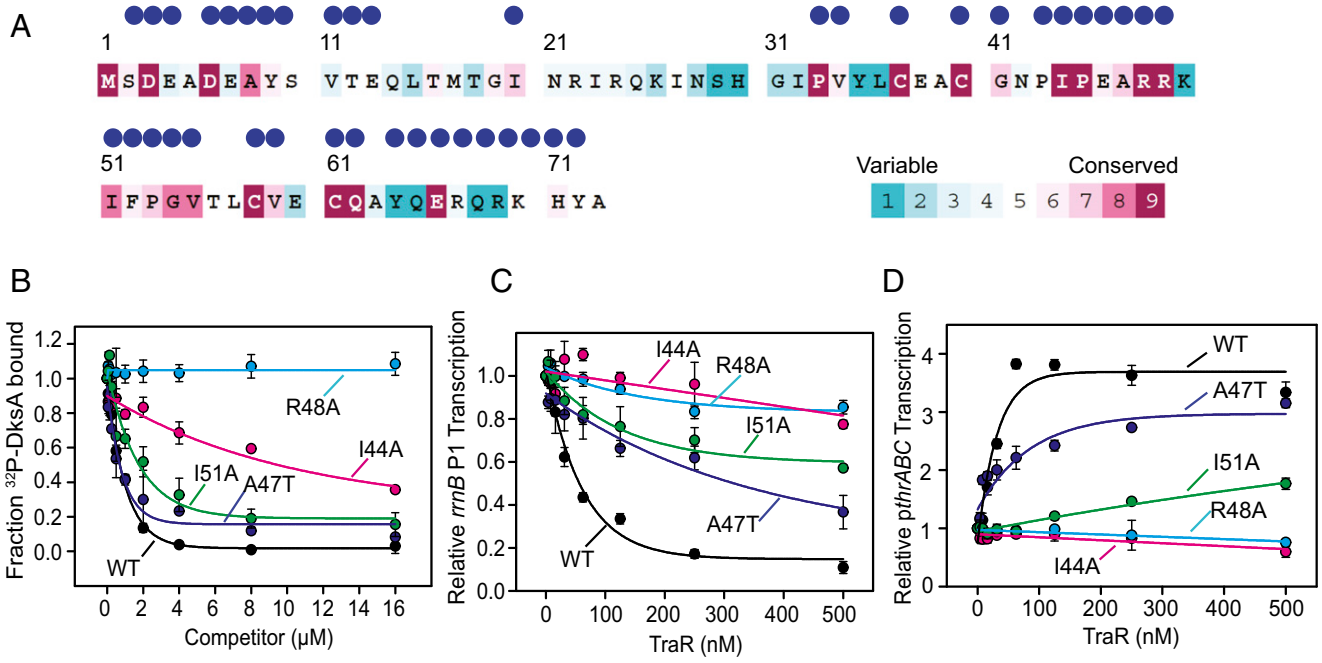

Fig. 7. Conservation of TraR and effects of globular domain substitutions on TraR function. (*A*) ConSurf Server (consurf.tau.ac.il/2016/) analysis of TraR residues conserved in a group of 100 TraR homologs of similar length from bacteriophage, plasmid, and bacterial sources (Table S2). Color key (degree of conservation) is at right. Dots indicate positions tested for complementation of a Δ*dksA* mutation in vivo (Table S1). (*B*) Binding by WT TraR and TraR variants to WT RNAP by competition with ^{32}P-DksA by Fe^{2+} -mediated cleavage as in Fig. 5*B*; 0.6 μM WT TraR, 0.7 μM A47T, 1.8 μM I51A TraR, or 9.8 μM I44A TraR reduced cleavage of bound ^{32}P-DksA by ∼50%. R48A TraR did not compete at any of the concentrations tested ($n = 2$). (*C*) Inhibition of *rrnB* P1 transcription by WT TraR and TraR variants as in Fig. 5*C*. IC_{50} = ∼55 nM for WT TraR, >4 μM for I44A and R48A, ∼310 nM for A47T, ∼545 nM for I51A. (*D*) Activation of the *thrABC* promoter as in Fig. 5*D* with WT TraR and TraR variants ($n = 2$).

cellular protein in uninduced cells. Additional studies will be needed to determine the TraR concentration and its physiological consequences when TraR is made from the Py promoter and DksA is present. Whatever the TraR concentration is during conjugation, we note that single-molecule studies suggest that the short residence time of secondary channel binding factors on RNAP helps them cooperate to regulate transcription while minimizing mutual interference (38).

The conservation of TraR homologs across major bacteriophage and bacterial groups suggests that its regulatory functions are strongly selected for in evolution. In general, ppGpp does not target RNAP directly in species distant from the proteobacteria (14). Thus, it is conceivable that TraR-like proteins have taken on some of the functions of ppGpp/DksA in the nonproteobacteria. Future characterization of the function of TraR homologs encoded by other conjugal plasmids, mobile elements, or bacteriophage may shed light on the roles of these factors in horizontal gene transfer.

Materials and Methods

Additional details for all procedures are in *SI Materials and Methods*.

Strains, Plasmids, Oligonucleotides, and Geneblock Sequences. Strains and plasmids are listed in Table S3, oligonucleotide sequences are in Table S4, and Geneblock (gBlock) sequences are in Table S5.

Purification of TraR, DksA, and RNAP. TraR and variants were purified from BL21DE3 *dksA*::Tn10 containing pET28a-*traR*-His6 plasmids by Ni-NTA chromatography (Qiagen) essentially as described previously (11). The histidine tag was cleaved off, and TraR without the His6 tag was dialyzed against storage buffer containing 10 mM Tris·Cl (pH 8.0), 0.1 mM EDTA, 2 mM DTT, 250 mM NaCl, and 50% glycerol. Protein concentrations were determined with the Bradford assay reagent (Bio-Rad) using BSA as a standard. HMK-DksA was purified as described previously (5). WT RNAP (core and holoenzyme), Bpa-containing RNAPs, and RNAPs not containing Bpa were purified as described previously (14, 35, 39).

In Vitro Transcription. Single- or multiple-round in vitro transcription reactions were carried out as described previously (5, 14). Reactions contained TraR, DksA, or ppGpp (TriLink Biotechnologies) at the concentrations indicated in the figure legends.

DNaseI Footprinting. DNaseI footprints were performed as described previously (35). Five-nanomolars of RNAP were added to ^{32}P-dCTP (Perkin-Elmer) end-labeled DNA in buffer containing 30 mM KCl, 10 mM Tris·Cl, pH 8.0, 10 mM $MgCl_2$, 1 mM DTT, and 0.1 mg/mL BSA.

^{32}P-ppGpp Binding Assay. The DRaCALA assay, adapted from ref. 27, was used to measure ^{32}P-ppGpp binding to proteins essentially as described previously (14), with WT or Δω RNAP, ±TraR or DksA.

Site-Directed Mutagenesis. Substitutions were introduced into pTrc99a-*traR* and/or pET28a-*traR* using the QuikChange Lightning Multi Site-Directed Mutagenesis Kit (Agilent) with mutagenic primers listed in Table S4. Mutations were confirmed by DNA sequencing.

Bpa Cross-Linking. Cross-linking was performed as described previously (16, 35) using ^{32}P-labeled HMK-DksA and ^{32}P-labeled TraR-HMK.

TraR–RNAP Binding (Fe^{2+} Cleavage Competition Assay). TraR (or DksA) binding to RNAP was determined by competition with ^{32}P-labeled DksA binding to RNAP. ^{32}P-labeled DksA binding to RNAP was detected by cleavage with hydroxyl radicals generated by Fe^{2+} in the RNAP active site, as described previously (22).

Western Blotting. Western blots were performed using standard procedures using a rabbit polyclonal anti-TraR antibody (Covance Research Product).

TraR Conservation Analysis. TraR-like proteins were identified by National Center for Biotechnology Information (NCBI) Blast using *E. coli* F plasmid-encoded TraR as a query. One-hundred different TraR homologs between

69 and 75 amino acids in length, representing a range of bacteria and bacteriophages, were chosen from ~500 TraR-like sequences, aligned using Clustal Omega, and analyzed for conservation of individual residues using the ConSurf Server (consurf.tau.ac.il/2016/) (Table S2). Degree of conservation is indicated in Fig. 7*A*. TraR homologs were identified in Proteobacteria, as well as distantly related species in Nitrospira, Bacilli, and Actinobacteria. The database annotations suggest that many of these sequences are in conjugal plasmids, prophage, or mobile elements. Among bacteriophages, TraR-like proteins were found in the Myoviridae, Siphoviridae, and Podoviridae families.

Modeling of TraR Bound to RNAP. A model for the structure of TraR was generated using RaptorX (raptorx.uchicago.edu/StructurePrediction/predict/). All 73 TraR residues were modeled. Six (8%) were predicted as disordered, and the secondary structure was predicted to contain 61% helix, 2% β-sheet, and 35% loop (Fig. 6*A*). The TraR–RNAP model was generated in Pymol based on genetic and biochemical data presented here and on models for how DksA binds in the secondary channel of RNAP (14, 17). The N-terminal region of TraR (including residues D3, D6, and A8) was aligned in PyMol with the coiled-coil tip region of DksA (Fig. 6*B*). TraR was positioned manually, because limited sequence similarity in the TraR N-terminal region precluded a Pymol-generated alignment.

Inductively Coupled Plasma-Mass Spectrometry Analysis. Elemental analysis of a purified TraR preparation for determination of zinc content was performed at the University of Wisconsin–Madison Soil & Plant Analysis Laboratory, Department of Soil Science.

Sedimentation Equilibrium Analytical Ultracentrifugation. The oligomeric state of purified TraR was determined by the University of Wisconsin–Madison Biophysics Instrumentation Facility.

ESI-Mass Spectrometry. ESI-mass spectrometry was performed by the Mass Spectrometry/Proteomics Facility in the Biotechnology Center, University of Wisconsin–Madison to determine the molecular mass of TraR and its oligomeric state.

ACKNOWLEDGMENTS. We thank Karen Wasserman for help with antibody production; Navneet Singh for preliminary Western blot analysis of TraR variants; Suzanne Treml for strain constructions; and Christophe Herman for helpful discussions. This work was supported by NIH Grant R37 GM37048 (to R.L.G.).

1. Liu X, Jiang H, Gu Z, Roberts JW (2013) High-resolution view of bacteriophage lambda gene expression by ribosome profiling. *Proc Natl Acad Sci USA* 110:11928–11933.
2. Storz G, Wolf YI, Ramamurthi KS (2014) Small proteins can no longer be ignored. *Annu Rev Biochem* 83:753–777.
3. Maneewannakul K, Ippen-Ihler K (1993) Construction and analysis of F plasmid *traR*, *trbJ*, and *trbH* mutants. *J Bacteriol* 175:1528–1531.
4. Blankschien MD, et al. (2009) TraR, a homolog of a RNAP secondary channel interactor, modulates transcription. *PLoS Genet* 5:e1000345.
5. Paul BJ, et al. (2004) DksA: A critical component of the transcription initiation machinery that potentiates the regulation of rRNA promoters by ppGpp and the initiating NTP. *Cell* 118:311–322.
6. Perederina A, et al. (2004) Regulation through the secondary channel—Structural framework for ppGpp-DksA synergism during transcription. *Cell* 118:297–309.
7. Paul BJ, Berkmen MB, Gourse RL (2005) DksA potentiates direct activation of amino acid promoters by ppGpp. *Proc Natl Acad Sci USA* 102:7823–7828.
8. Doran TJ, Loh SM, Firth N, Skurray RA (1994) Molecular analysis of the F plasmid traVR region: traV encodes a lipoprotein. *J Bacteriol* 176:4182–4186.
9. Sergueev K, Court D, Reaves L, Austin S (2002) *E. coli* cell-cycle regulation by bacteriophage lambda. *J Mol Biol* 324:297–307.
10. Frost LS, Ippen-Ihler K, Skurray RA (1994) Analysis of the sequence and gene products of the transfer region of the F sex factor. *Microbiol Rev* 58:162–210.
11. Grace ED, et al. (2015) Activation of the σE-dependent stress pathway by conjugative TraR may anticipate conjugational stress. *J Bacteriol* 197:924–931.
12. Ross W, Vrentas CE, Sanchez-Vazquez P, Gaal T, Gourse RL (2013) The magic spot: A ppGpp binding site on *E. coli* RNA polymerase responsible for regulation of transcription initiation. *Mol Cell* 50:420–429.
13. Zuo Y, Wang Y, Steitz TA (2013) The mechanism of *E. coli* RNA polymerase regulation by ppGpp is suggested by the structure of their complex. *Mol Cell* 50:430–436.
14. Ross W, et al. (2016) ppGpp binding to a site at the RNAP-DksA interface accounts for its dramatic effects on transcription initiation during the stringent response. *Mol Cell* 62:811–823.
15. Rutherford ST, et al. (2007) Effects of DksA, GreA, and GreB on transcription initiation: Insights into the mechanisms of factors that bind in the secondary channel of RNA polymerase. *J Mol Biol* 366:1243–1257.
16. Lennon CW, et al. (2012) Direct interactions between the coiled-coil tip of DksA and the trigger loop of RNA polymerase mediate transcriptional regulation. *Genes Dev* 26:2634–2646.
17. Parshin A, et al. (2015) DksA regulates RNA polymerase in *Escherichia coli* through a network of interactions in the secondary channel that includes sequence insertion 1. *Proc Natl Acad Sci USA* 112:E6862–E6871.
18. Laptenko O, Lee J, Lomakin I, Borukhov S (2003) Transcript cleavage factors GreA and GreB act as transient catalytic components of RNA polymerase. *EMBO J* 22:6322–6334.
19. Opalka N, et al. (2003) Structure and function of the transcription elongation factor GreB bound to bacterial RNA polymerase. *Cell* 114:335–345.
20. Lamour V, et al. (2008) Crystal structure of *Escherichia coli* Rnk, a new RNA polymerase-interacting protein. *J Mol Biol* 383:367–379.
21. Lemke JJ, et al. (2011) Direct regulation of *Escherichia coli* ribosomal protein promoters by the transcription factors ppGpp and DksA. *Proc Natl Acad Sci USA* 108: 5712–5717.
22. Lennon CW, Gaal T, Ross W, Gourse RL (2009) *Escherichia coli* DksA binds to free RNA polymerase with higher affinity than to RNA polymerase in an open complex. *J Bacteriol* 191:5854–5858.
23. Rutherford ST, Villers CL, Lee JH, Ross W, Gourse RL (2009) Allosteric control of *Escherichia coli* rRNA promoter complexes by DksA. *Genes Dev* 23:236–248.
24. Barker MM, Gaal T, Gourse RL (2001) Mechanism of regulation of transcription initiation by ppGpp. II. Models for positive control based on properties of RNAP mutants and competition for RNAP. *J Mol Biol* 305:689–702.
25. Repoila F, Gottesman S (2001) Signal transduction cascade for regulation of RpoS: Temperature regulation of DsrA. *J Bacteriol* 183:4012–4023.
26. Bougdour A, Gottesman S (2007) ppGpp regulation of RpoS degradation via anti-adaptor protein IraP. *Proc Natl Acad Sci USA* 104:12896–12901.
27. Roelofs KG, Wang J, Sintim HO, Lee VT (2011) Differential radial capillary action of ligand assay for high-throughput detection of protein-metabolite interactions. *Proc Natl Acad Sci USA* 108:15528–15533.
28. Satory D, Halliday JA, Sivaramakrishnan P, Lua RC, Herman C (2013) Characterization of a novel RNA polymerase mutant that alters DksA activity. *J Bacteriol* 195: 4187–4194.
29. Lee JH, Lennon CW, Ross W, Gourse RL (2012) Role of the coiled-coil tip of *Escherichia coli* DksA in promoter control. *J Mol Biol* 416:503–517.
30. Blankschien MD, et al. (2009) Super DksAs: Substitutions in DksA enhancing its effects on transcription initiation. *EMBO J* 28:1720–1731.
31. Källberg M, et al. (2012) Template-based protein structure modeling using the RaptorX web server. *Nat Protoc* 7:1511–1522.
32. Ashkenazy H, Erez E, Martz E, Pupko T, Ben-Tal N (2010) ConSurf 2010: Calculating evolutionary conservation in sequence and structure of proteins and nucleic acids. *Nucleic Acids Res* 38:W529–W533.
33. Furman R, Tsodikov OV, Wolf YI, Artsimovitch I (2013) An insertion in the catalytic trigger loop gates the secondary channel of RNA polymerase. *J Mol Biol* 425:82–93.
34. Mekler V, Minakhin L, Borukhov S, Mustaev A, Severinov K (2014) Coupling of downstream RNA polymerase-promoter interactions with formation of catalytically competent transcription initiation complex. *J Mol Biol* 426:3973–3984.
35. Winkelman JT, et al. (2015) Crosslink mapping at amino acid-base resolution reveals the path of DNA in a scrunched initial transcribing complex. *Mol Cell* 59:768–780.
36. Frost LS, Manchak J (1998) F-phenocopies: Characterization of expression of the F transfer region in stationary phase. *Microbiology* 144:2579–2587.
37. Murray HD, Schneider DA, Gourse RL (2003) Control of rRNA expression by small molecules is dynamic and nonredundant. *Mol Cell* 12:125–134.
38. Tetone LE, et al. (2017) Dynamics of GreB-RNA polymerase interaction allow a proofreading accessory protein to patrol for transcription complexes needing rescue. *Proc Natl Acad Sci USA* 114:E1081–E1090.
39. Burgess RR, Jendrisak JJ (1975) A procedure for the rapid, large-scall purification of *Escherichia coli* DNA-dependent RNA polymerase involving polymin P precipitation and DNA-cellulose chromatography. *Biochemistry* 14:4634–4638.
40. Chin JW, Martin AB, King DS, Wang L, Schultz PG (2002) Addition of a photocrosslinking amino acid to the genetic code of *Escherichia coli*. *Proc Natl Acad Sci USA* 99:11020–11024.
41. Amann E, Ochs B, Abel KJ (1988) Tightly regulated *tac* promoter vectors useful for the expression of unfused and fused proteins in *Escherichia coli*. *Gene* 69:301–315.
42. Winkelman JT, Chandrangsu P, Ross W, Gourse RL (2016) Open complex scrunching before nucleotide addition accounts for the unusual transcription start site of *E. coli* ribosomal RNA promoters. *Proc Natl Acad Sci USA* 113:E1787–E1795.